

OGLE-2011-BLG-0417: A Radial Velocity Testbed for Microlensing

Andrew Gould¹, In-Gu Shin², Cheongho Han², Andrzej Udalski³, Jennifer C. Yee¹

ABSTRACT

Microlensing experiments are returning increasingly detailed information about the planetary and binary systems that are being detected, far beyond what was originally expected. In several cases the lens mass and distance are measured, and a few very special cases have yielded complete 8-parameter Kepler solutions, i.e., the masses of both components, five Kepler invariants and the phase. We identify one such case that is suitable for a precision test that could be carried out by comparing Doppler (RV) measurements with the predictions from the microlensing solution. The lens primary is reasonably bright ($I = 16.3$, $V = 18.0$) and is expected to have a relatively large RV semi-amplitude ($K \sim 6.35 \text{ km s}^{-1}$).

Subject headings: gravitational lensing: micro — binaries: general — techniques: radial velocities

1. Introduction

When microlensing planet searches were first proposed (Liebes 1964; Mao & Paczyński 1991; Gould & Loeb 1992) it was not expected that much information would be extracted about the individual planets that were detected. Gould & Loeb (1992) pointed out that the planet-host mass ratio q and the planet-host projected separation s in units of the Einstein radius can be measured, but no other parameter measurements were mentioned. By contrast, Doppler (RV) detections routinely return six independent parameters out of the eight possible, i.e., the masses of the two bodies, plus six phase-space coordinates. The latter are usually parameterized by five Kepler-orbit invariants plus the orbital phase. After

¹Department of Astronomy, Ohio State University, 140 W. 18th Ave., Columbus, OH 43210, USA; gould@astronomy.ohio-state.edu

²Department of Physics, Chungbuk National University, Cheongju 361-763, Korea

³Warsaw University Observatory, Al. Ujazdowskie 4, 00-478 Warszawa, Poland

one includes a spectroscopic determination of the host mass, RV lacks only the orientation of the orbit on the plane of the sky (which is generally of little interest) and resolution of the famous $m \sin i$ degeneracy, where m is the planet mass and i is the orbital inclination.

However, over the course of two decades, our understanding of what can be extracted from microlensing planet and binary detections has gradually expanded to the point that now, incredibly, sometimes all eight parameters are reported. There only remains a single discrete degeneracy: the sign of the radial velocity.

First, if the source passes over a caustic caused by the lens, one can measure the angular size of the source relative to the Einstein ring, $\rho = \theta_*/\theta_E$ (Gould 1994; Witt & Mao 1994; Nemiroff & Wickramasinghe 1994). The very first microlensing planet OGLE-2003-BLG-235Lb showed such “finite-source effects” (Bond et al. 2004), and indeed the majority of subsequent microlensing planets have as well. Since θ_* can be measured from an instrumental color magnitude diagram (CMD) of the event (Yoo et al. 2004) and such color data are routinely taken, the majority of events also yield θ_E . Gould (1992) pointed out that the “microlens parallax” π_E could in principle be measured from lightcurve distortions due to Earth’s motion, and that if both π_E and θ_E could be measured, then so could the lens mass. Here,

$$\theta_E^2 = \kappa M \pi_{\text{rel}}; \quad \pi_E^2 = \frac{\theta_E}{\kappa M}; \quad \kappa \equiv \frac{4G}{c^2 \text{AU}} \simeq 8.1 \frac{\text{mas}}{M_\odot}, \quad (1)$$

M is the total mass of the lens, and $\pi_{\text{rel}} \equiv \pi_L - \pi_S$ is the lens-source relative parallax. Already, the second microlensing planet OGLE-2005-BLG-071 (Udalski et al. 2005) showed such parallax distortions, and thus became the first microlensing planet with a mass measurement (Dong et al. 2009). A substantial minority of subsequent microlensing planets yielded microlens parallax measurements as well. Since, the source distance (and so $\pi_S = \text{AU}/D_S$) is usually known quite well, Equation (1) also yields the lens distance D_L and so also the physical projected separation $r_\perp = s\theta_E D_L$. Since the microlens parallax measurement is actually described by a vector $\boldsymbol{\pi}_E$ (Gould 2004) whose direction is that of the lens-source relative motion, the projected separation \mathbf{r}_\perp in fact contains two phase-space coordinates.

This still leaves four phase-space coordinates to be determined for a complete orbital solution. It was an enormous surprise when the first orbital motion was derived from the microlensing event MACHO-BLG-97-041 (Albrow et al. 2000) because the perturbations due to the lens structure typically last a few days while the orbital periods are expected to be several years. Even then the measurement was considered highly unique, due to accidental geometry. Moreover, even in that exceptionally favorable circumstance, only two additional parameters were measured: the time rate of change of the binary separation ds/dt , which affects the shape of the caustic; and the time rate of change of the angular orientation of the lens axis, $\omega = d\alpha/dt$, which affects the orientation of the caustic. Hence, in this case, the four

phase-space coordinates in the plane of the sky were measured, and the two radial coordinates were not. This seems natural because microlensing is sensitive to the mass distribution projected along the line of sight. Several planetary events have yielded such measurements, or partial measurements, the first two being OGLE-2005-BLG-071 (Dong et al. 2009) and OGLE-2006-BLG-109 (Gaudi et al. 2008; Bennett et al. 2010).

Even as these measurements began to accumulate it was regarded as virtually impossible to obtain information about the orbit in the third direction, which would be the only way to derive the invariants of a Kepler orbit. And indeed, no such measurements have yet been made for planetary events. However, just as it is possible to use Kepler’s Second Law to deproject astrometric data on visual binaries to obtain a full orbit, it should in principle be possible to deproject microlensing-binary orbits. The challenge is, again, that the perturbations are generally short compared to an orbital period. Nevertheless, Skowron et al. (2011) analyzed the binary-lens event OGLE-2009-BLG-020 and found that two additional parameters were required to describe the event, s_z and γ_z , the position and time rate of change of the binary separation in the radial direction. That is, all six phase-space coordinates were needed. Now, in that particular case, the fits to these parameters were highly correlated (see their Figure 3). However, Skowron et al. (2011) took this opportunity to work out the relations of microlensing parameters and Kepler parameters (see their Appendices A and B). Then, making use of this formalism, Shin et al. (2011, 2012) were able to obtain complete (8-parameter) Kepler solutions for three events, OGLE-2005-BLG-018, MOA-2011-BLG-090, and OGLE-2011-BLG-0417. In this paper, we will show how the complete solution for OGLE-2011-BLG-0417 allows a direct test of the microlensing model.

2. Past Tests of Microlensing

The importance of these measurements goes far beyond what they tell us about the individual systems. Microlensing events are famously “unrepeatable”. This does not mean that the results cannot be corroborated, but it does pose challenges.

For example, few would doubt the basic interpretation of either of the two-planet systems discovered by microlensing, OGLE-2006-BLG-109Lb,c (Gaudi et al. 2008; Bennett et al. 2010) and OGLE-2012-BLG-0026Lb,c (Han et al. 2013). All the features of these observed events can be understood in terms of well-established (if specialized) microlensing principles. Several of the major features are corroborated by overlapping data sets. Nevertheless, there are aspects of the modeling of both events that yield nominally high signal-to-noise ratio parameter measurements without corresponding “visible and unambiguous” lightcurve features. In particular, both events yield microlens parallax measurements that have obvious signa-

tures for only one of the two components of the microlens parallax vector $\boldsymbol{\pi}_E = (\pi_{E,\parallel}, \pi_{E,\perp})$. That is, the component of $\boldsymbol{\pi}_E$ parallel to the projected position of the Sun ($\pi_{E,\parallel}$) leads to an obvious asymmetry in the light curve (Gould et al. 1994), while the signature of $\pi_{E,\perp}$ is entangled with many other lightcurve parameters, in particular ω , the component of lens orbital motion perpendicular to the binary axis (Batista et al. 2011; Skowron et al. 2011). Hence, it is not at all obvious that $\boldsymbol{\pi}_E$, and so $\pi_E = |\boldsymbol{\pi}_E|$, and thus M and D_L are being measured correctly.

In most cases, tests of these subtle higher-order microlensing parameter measurements are impossible. Fortunately, however, there are a few rare cases for which they are possible. Moreover, there are no obvious reasons that the events that can be tested are more likely to have correctly measured microlensing parameters than those that cannot.

The number of such tests that have been carried out in the past is actually quite small. In fact, there are just two. However, both were spectacular successes. The first was MACHO-LMC-5, an event that occurred in 1993, whose lightcurve yielded a measurement of $\boldsymbol{\pi}_E$ but not θ_E . However, $\Delta t = 6.3$ yr later, Alcock et al. (2001) imaged the lens and source using the *Hubble Space Telescope (HST)* and thereby found the lens-source relative proper motion $\boldsymbol{\mu} = \Delta\boldsymbol{\theta}/\Delta t$, where $\Delta\boldsymbol{\theta}$ is the vector separation between the lens and source stars. When combined with the Einstein timescale t_E measured from the event, this yielded $\theta_E = \mu t_E$. These measurements allowed for two tests. First, the photometry of the lens should have been consistent with the mass and distance inferred from the measurements of $\boldsymbol{\pi}_E$ (lightcurve) and θ_E (lightcurve plus *HST* astrometry). Second, the direction of $\boldsymbol{\mu}$ (*HST* astrometry) should have been the same as that of $\boldsymbol{\pi}_E$ (lightcurve). In fact, the observations appeared to fail both tests. Subsequently, however, Gould (2004) found a discrete degeneracy in the parallax solution, with the other solution yielding consistency for both tests. Moreover, Drake et al. (2004) obtained a trigonometric parallax for the lens and confirmed the alternative microlensing parallax derived by Gould (2004).

The second tested event was OGLE-2006-BLG-109, the first two-planet event. This event yielded both $\boldsymbol{\pi}_E$ and the transverse orbital parameters ds/dt and ω . Recall that $\pi_{E,\perp}$ can be entangled with ω as well as other parameters. The lens flux predicted on the basis of the mass and distance derived from $\boldsymbol{\pi}_E$ and θ_E was far smaller than the blended light superposed on the source. This could have either been because of errors in $\boldsymbol{\pi}_E$ and/or θ_E , or because there was additional light in the aperture, i.e., not related to either the source or lens of the event. Bennett et al. (2010) obtained AO images using the Keck telescope and found that the blended light was clearly displaced from the event and that the “object” at the location of the event was consistent with the combined light from the source and lens, as predicted by the microlens solution.

3. A New Test

However, to date, there has never been a test of microlensing orbital-parameter measurements. We here propose such a test. Of the three binary events with complete solutions, OGLE-2011-BLG-0417 is by far the best candidate. OGLE-2005-BLG-018 has an extremely bright source star, which would preclude making measurements of the lens star until the two separate by at least several hundred mas, many decades from now. The brighter component of MOA-2011-BLG-090L is expected to be $I \gtrsim 20.5$, making it virtually impossible to monitor at the required RV precision.

However, OGLE-2011-BLG-0417L is so bright, it is easily identified as the “blended light” in the event CMD (see Figure 4 of Shin et al. 2012). Indeed, the fact that this blended-light point sits right on the “disk main sequence” or “reddening track” at roughly the position expected for the primary component of the lens, is already an indication that the microlensing solution is basically correct. But because the lens is bright, $I_L \sim 16.3$, $V_L \sim 18.0$, it is also feasible to test whether the orbit as determined from the microlensing solution is correct.

Table 1 shows the eight Kepler parameters determined from microlensing (total mass, mass ratio, 5 Kepler invariants, and time of periastron), plus the lens distance, which is also determined. These are derived from the underlying Markov chains used by Shin et al. (2012) except that we have adopted the new bulge clump giant calibration of Nataf et al. (2012) and also have allowed for the 5% error in θ_* , which was not previously included. Note that in order to express the results as precisely as possible, the correlation coefficients are displayed, as well as the errors.

Table 2 shows our predictions (and covariance matrix) for the five Kepler parameters that can be measured by RV (velocity semi-amplitude, period, eccentricity, argument of periastron, time of periastron) as well as the primary mass and system distance, which can both be estimated from the spectrum (in the latter case augmented by calibrated photometry). In this case, it is especially important to state the correlation coefficient between the period and time of periastron, since the particular orbit when t_p will be measured is not known in advance.

Figure 1 shows the predicted RV curve over the next several years. It is virtually impossible to make observations within 45 days to the Winter Solstice. The resulting exclusion zones are marked in dashed lines. We also mark a more conservative window of ± 75 days from the Winter Solstice. Note that while the *form* of the RV curve is well-predicted, the *phase* is gradually being lost. The error bar in the figure indicates the uncertainty in the time of the first periastron. Because of the high eccentricity, this phase can be recaptured

by a few judiciously placed RV observations.

The predicted RV amplitude ($K = 6.35 \pm 0.34, \text{ km s}^{-1}$) is relatively high and should be measurable with good precision, despite the relatively faint (for typical RV work) target, $I \sim 16.3, V \sim 18.0$. One complicating factor is that (as with all microlensing events), the lens is superposed on the source, which in this case is a clump giant. However, because the source is almost 10 times more distant and is seen through $\Delta E(V - I) \sim 1$ mag more reddening, the lens is actually brighter than the source by about 0.4 mag in I and 1.3 mag in V . See Figure 4 of Shin et al. (2012). Moreover, given that the lens is in the Galactic Disk whereas the source is in the Bulge, they are likely to have RVs that differ by several tens of km s^{-1} .

4. Conclusion

We have proposed a rigorous test of microlensing parameters via RV measurements of OGLE-2011-BLG-0417L, a binary lens with a complete orbital solution. The expected RV semi-amplitude is $6.35 \pm 0.34 \text{ km s}^{-1}$, which should be precisely measurable despite the fact that the lens primary is relatively faint ($I = 16.3, V = 18.0$) and is superposed on a somewhat fainter star that was the source star in the microlensing event. We have presented both the predicted values and error bars of all seven quantities that are measurable with RV, including 5 Kepler parameters (or parameter combinations), the primary mass (from spectroscopic typing) and the distance (from combined spectroscopy and photometry).

This would be only the third precision test of microlensing by external measurements, and would be by far the most exacting, since many more parameter determinations would be tested in a much more complicated system.

AG was supported by NSF grant AST 1103471. Work by CH was supported by Creative Research Initiative Program (2009-0081561) of National Research Foundation of Korea. The OGLE project has received funding from the European Research Council under the European Community's Seventh Framework Programme (FP7/2007-2013) / ERC grant agreement no. 246678 to AU. Work by JCY was supported by an NSF Graduate Research Fellowship under Grant No. 2009068160.

REFERENCES

Albrow, M.D., Beaulieu, J.-P., Caldwell, J.A.R. 2000, ApJ, 534, 894

- Alcock, C., Allsman, R.A., Alves, D.R. et al. 2001, *Nature*, 414, 617
- Batista, V., Gould, A., Dieters, S. et al. 2011, *A&A*, 529,110
- Bennett, D.P., Rhie, S.H., Nikolaev, S. et al. 2010, *ApJ*, 713, 837
- Bond, I.A., Udalski, A., Jaroszyński, M. et al. 2004, *ApJ*, 606, L155
- Drake, A.J., Cook, K.H., & Keller, S.C. 2004, *ApJ*607 L29
- Han, C., Udalski, A., Choi, J.-Y. et al. 2013, *ApJ*, 762, L28
- Dong, S., Gould, A., Udalski, A. et al. 2009, *ApJ*, 695, 970
- Gaudi, B.S., Bennett, D.P., Udalski, A. et al. 2008, *Science*, 319, 927
- Gould, A. 1992, *ApJ*, 392, 442
- Gould, A. 1994, *ApJ*, 421, L71
- Gould, A. 2004, *ApJ*, 606, 319
- Gould, A., & Loeb, A. 1992, *ApJ*, 396, 104
- Gould, A., Miralda-Escudé & Bahcall, J.N. 1994, *ApJ*, 423, L105
- Liebes, S. 1964, *Physical Review*, 133, 835
- Mao, S. & Paczyński, B. 1991, *ApJ*, 374, L37
- Nataf, D.M., Gould, A., Fouqué, P. et al. 2012, *ApJ*, submitted, arXiv:1208:1263
- Nemiroff, R.J., & Wickramasinghe, W.A.D.T. 1994, *ApJ*, 424, L21
- Shin, I.-G., Udalski, A., Han, C. et al. 2011, *ApJ*, 735, 85
- Shin, I.-G., Han, C., Choi, J.-Y., et al. 2012, *ApJ*, 755, 91
- Skowron, J., Udalski, A., Gould, A et al. 2011, *ApJ*, 738, 87
- Udalski, A., Jaroszyński, M., Paczyński, B., et al. 2005, *ApJ*, 628, L109
- Witt, H.J., & Mao, S. 1994, *ApJ*, 429, 66
- Yoo, J., DePoy, D.L., Gal-Yam, A. et al. 2004, *ApJ*, 603, 139

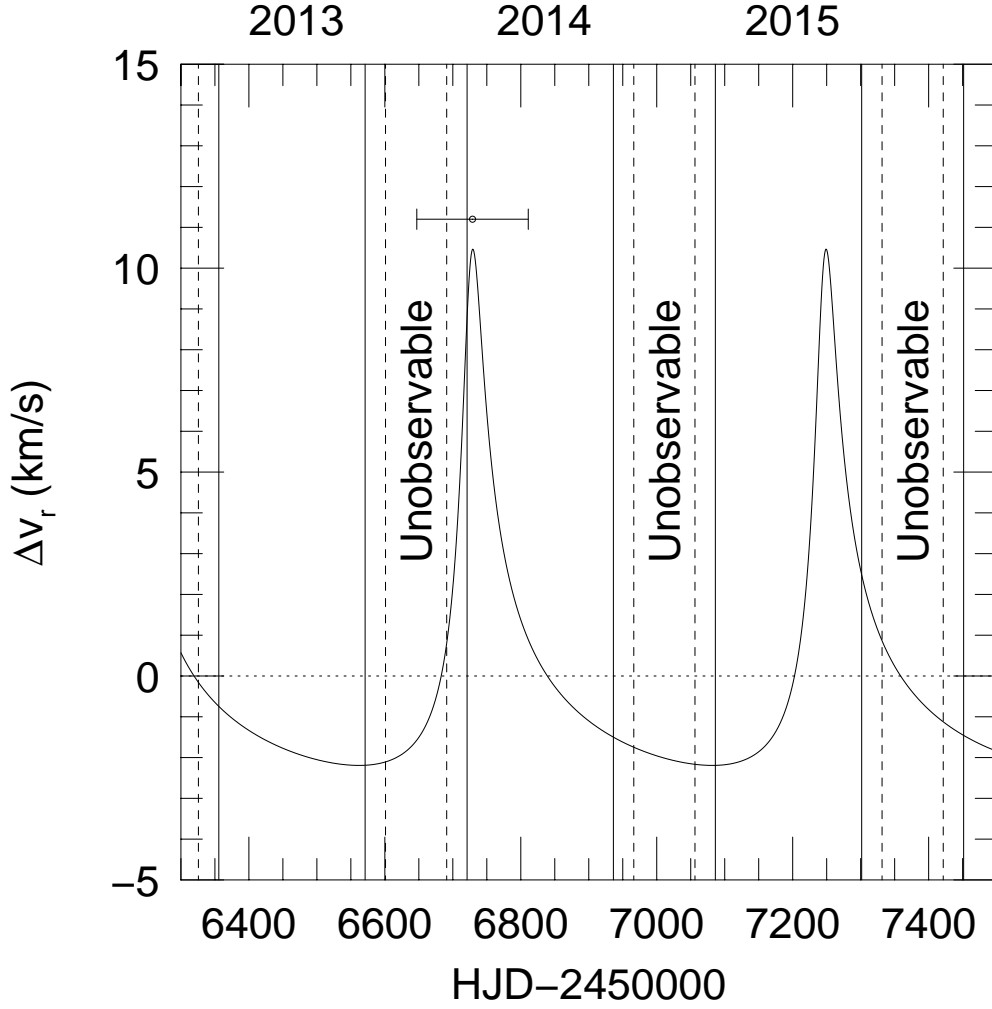


Fig. 1.— Predicted RV curve for the primary of OGLE-2011-BLG-0417L, based on the analysis of Shin et al. (2012). Dashed lines indicate ± 45 days from the winter Solstice, when observations are virtually impossible from Earth. Solid lines show a more conservative exclusion window of ± 75 days. Note that microlensing predictions are intrinsically ambiguous as to the sign of the RV curve. While the *form* of this curve is well-predicted, the *phase* is gradually being lost: the error bar at the first periastron indicates the phase error at that time. RV observations can easily recover the phase.

Table 1: MICROLENS MEASUREMENTS

	M_{tot}	M_2/M_1	P	e	i	ω	Ω	t_{peri}	D_L
	(M_{\odot})		(yr)		(deg)	(deg)	(deg)	(HJD)	(kpc)
Value	0.677	0.292	1.423	0.688	60.963	341.824	125.374	5686.344	0.951
Error	0.047	0.003	0.113	0.027	1.554	2.655	1.649	6.960	0.058
C.C.	1.000	-0.204	0.101	0.511	-0.024	-0.008	0.511	0.133	-0.065
C.C.	-0.204	1.000	-0.055	-0.150	0.161	-0.065	-0.302	-0.015	-0.136
C.C.	0.101	-0.055	1.000	-0.118	0.523	0.484	0.595	-0.756	0.791
C.C.	0.511	-0.150	-0.118	1.000	-0.217	-0.247	0.151	0.485	0.211
C.C.	-0.024	0.161	0.523	-0.217	1.000	-0.257	0.141	-0.781	0.093
C.C.	-0.008	-0.065	0.484	-0.247	-0.257	1.000	0.667	-0.013	0.518
C.C.	0.511	-0.302	0.595	0.151	0.141	0.667	1.000	-0.141	0.469
C.C.	0.133	-0.015	-0.756	0.485	-0.781	-0.013	-0.141	1.000	-0.367
C.C.	-0.065	-0.136	0.791	0.211	0.093	0.518	0.469	-0.367	1.000

Table 2: PREDICTIONS FOR RV MEASUREMENTS

	K	P	e	ω	t_{peri}	M_1	D_L
	(km s^{-1})	(yr)		(deg)	(HJD)	(M_{\odot})	(kpc)
Value	6.352	1.423	0.688	341.824	5686.344	0.524	0.951
Error	0.340	0.113	0.027	2.655	6.960	0.036	0.058
C.C.	1.000	-0.365	0.838	-0.473	0.503	0.693	-0.267
C.C.	-0.365	1.000	-0.118	0.484	-0.756	0.101	0.791
C.C.	0.838	-0.118	1.000	-0.247	0.485	0.511	0.211
C.C.	-0.473	0.484	-0.247	1.000	-0.013	-0.008	0.518
C.C.	0.503	-0.756	0.485	-0.013	1.000	0.133	-0.367
C.C.	0.693	0.101	0.511	-0.008	0.133	1.000	-0.065
C.C.	-0.267	0.791	0.211	0.518	-0.367	-0.065	1.000